Arch Environ Contam Toxicol (2015) 69:20–31
DOI 10.1007/s00244-015-0144-9

# Multiple Factors Affect Diversity and Abundance of Ammonia-Oxidizing Microorganisms in Iron Mine Soil

Yi Xing[1] · Yan-Xiao Si[1] · Chen Hong[1,2] · Yang Li[1]

Received: 23 August 2014 / Accepted: 28 February 2015 / Published online: 10 April 2015
© Springer Science+Business Media New York 2015

**Abstract** Ammonia oxidation by microorganisms is a critical process in the nitrogen cycle. In this study, four soil samples collected from a desert zone in an iron-exploration area and others from farmland and planted forest soil in an iron mine surrounding area. We analyzed the abundance and diversity of ammonia-oxidizing archaea (AOA) and ammonia-oxidizing bacteria (AOB) in iron-mining area near the Miyun reservoir using ammonia monooxygenase. A subunit gene (*amo*A) as molecular biomarker. Quantitative polymerase chain reaction was applied to explore the relationships between the abundance of AOA and AOB and soil physicochemical parameters. The results showed that AOA were more abundant than AOB and may play a more dominant role in the ammonia-oxidizing process in the whole region. PCR-denaturing gradient gel electrophoresis was used to analyze the structural changes of AOA and AOB. The results showed that AOB were much more diverse than AOA. *Nitrosospira* cluster three constitute the majority of AOB, and AOA were dominated by group 1.1b in the soil. Redundancy analysis was performed to explore the physicochemical parameters potentially important to AOA and AOB. Soil characteristics (i.e. water, ammonia, organic carbon, total nitrogen, available phosphorus, and soil type) were proposed to potentially contribute to the distributions of AOB, whereas Cd was also closely correlated to the distributions of AOB. The community of AOA correlated with ammonium and water contents. These results highlight the importance of multiple drivers in microbial niche formation as well as their affect on ammonia oxidizer composition, both which have significant consequences for ecosystem nitrogen functioning.

Long-term open-pit mining, screening, and crushing ore releases large amounts of industrial dust. Tailing sands and iron deposit rocks are mostly stacked directly on the ground in China. These minerals, which contain heavy metals—e.g., copper (Cu), zinc (Zn), lead (Pb), chromium (Cr), cadmium (Cd), nickel (Ni), and cobalt (Co)—easily cause potential risk to human health and ecosystems through wind force and surface runoff into surrounding soils (Zhou et al. 2015). Compared with soil biomass, soil respiration, enzyme activity, and nitrogen (N) fixation, which can be used to assess the effect of heavy metals on soil microbial communities, nitrification is one of the most sensitive soil microbial processes for heavy-metal stress (Broos et al. 2005). Moreover, nitrification is an important process of soil nitrogen transformation. Nitrification is divided into two steps: $NH_3 \rightarrow NO_2^-$ (ammonia oxidation) and $NO_2^- \rightarrow NO_3^-$ (nitrite oxidation), and the former is a rate-limiting step and plays a critical role in the global nitrogen cycle. AOB or AOA were verified to have critical roles based on a series of surveys of soil ecosystems for

**Electronic supplementary material** The online version of this article (doi:10.1007/s00244-015-0144-9) contains supplementary material, which is available to authorized users.

✉ Chen Hong
hongchen000@126.com

Yi Xing
xingyi204@gmail.com; xingyi@ustb.edu.cn

[1] School of Civil and Environmental Engineering, and Key Laboratory of Metal and Mine Efficiently Exploiting and Safety, Ministry of Education, University of Science and Technology Beijing, Xueyuan Road No.30, Haidian District, Beijing 100083, China

[2] Research Center for Eco-Environmental Science, Chinese Academy of Sciences, Shuangqing Road No. 18, Haidian District, Beijing 100085, China

contribution to the nitrogen cycle (Kelly et al. 2011; Qin et al. 2013; Sher et al. 2013).

Several studies have indicated that AOA dominate the nitrification process in acidic, low-nutrient soils, whereas AOB dominate in neutral, alkaline, and N-rich soils (Erguder et al. 2009; Shen et al. 2012).Other studies discovered that bacteria rather than archaea dominate the microbial ammonia oxidation in particular farmland and grassland soil (Di et al. 2009; Jia and Conrad 2009). Furthermore, many researchers found that soil physical and chemical properties, such as pH, temperature, moisture, substrate concentration, soil types, and land-use types, played important roles in niche separation between AOA and AOB (Gubry-Rangin et al. 2011; O'Sullivan et al. 2013; Placella and Firestone 2013; Verhamme et al. 2011; Yao et al. 2013). In addition to the influence of soil properties, heavy metal, which has turned out to be a key factor in regulating microbial nitrogen cycle (Morel and Price 2003), could exert effects on ammonia oxidizers. Recently, Mertens and Ruyters showed that soil AOB seems more tolerant to Zn contamination than AOA several years after a single Zn application (Mertens et al. 2009; Ruyters et al. 2013). Liu showed that the community structure of AOA and AOB was suppressed in varying degrees under heavy-metal pollution in a rice field (Liu et al. 2014). So far, most studies have focused on the effects of either soil properties or heavy-metal pollution, whereas the methods by which the heavy-metal and soil properties work together on ammonia-oxidizing microorganism are not well understood.

The present study was performed in iron area of Chaohe River basin, which has rich iron ore resources and a mining history of >30 years, located in north of Miyun County, Beijing City, China 10 km upstream of the Miyun Reservoir. In this study, the *amo*A gene was applied as a molecular marker to investigate the community structure of ammonia oxidizer by denaturing gradient gel electrophoresis (DGGE) and the abundance by quantitative polymerase chain reaction (q-PCR). We further studied the possible link between *amo*A gene and potential ammonia oxidization (PAO) to illustrate the role of ammonia oxidizer in nitrification. Statistical analyses were also employed to correlate these results with physicochemical parameters, including heavy metals and soil properties, to identify the potential contributors to AOA and AOB.

## Materials and Methods

### Soil Sample Collection

In October 2012, 14 surface soils (0–20-cm deep) were sampled in four iron mines, named Fangmayu-Anzigou (FD), Sangyuan (SD), Xiaocaocun (XD), and Heiguyan (HD), of Chaohe basin. Four samples (FD, SD, XD, HD) came from the desert in an iron-exploration area. Ten samples were taken from sites A through E in area surrounding an iron mine and consisted of farmland and planted forest soil in every site. The coordinates of sampling sites A through E
are 40 35′45.87″N 117 8′21.74″E; 40 34′50.97″N 117 8′8.04″E; 40 34′25.06″N 117 9′45.57″E; 40 33′27.01″N 117 8′21.26″E; 40 32′27.84″N 117 7′and 39.70″E. Each sample was 1 kg in weight, was combined with four subsamples within an area of 5 × 5 $m^2$, and was then reduced to approximately 1 kg after sample quartering in the field. Samples were packed in sterile zip-lock bags, which were sealed and transported to the laboratory for further study. A fraction of the mixed sample was stored at 20 °C for subsequent molecular analysis. Another fraction was dried at room temperature for 1 week and sieved over a 4-mm grid to remove the stones and plants. One aliquot was then threaded through a 2-mm sieve to determine pH and available phosphorus, and the others were passed through a 0.125-m sieve to determine organic C (Corg), total nitrogen (Nt), and other metal contents. All samples were stored at 4 °C.

### Assays of Soil Properties, Heavy Metals, and Potential Ammonia Oxidation

All samples were analyzed for pH, water content (WC), Corg, Nt, available phosphorus, and heavy metals. WC in samples was determined immediately after collection by drying at 105 °C until constant weight. The pH was determined with a pH meter (Starter-3C, OHAUS, USA) in a 1:2.5 suspension of ultrapure water. Corg was determined with a 2400II CHNS/O elemental analyzer (Perkin-Elmer, USA) after removing the inorganic C by digesting in 1 M HCl for 48 h, washing with ultrapure water until becoming neutral and drying at low temperature. Nt was directly detected using a CHNS/O elemental analyzer. Soil samples were extracted by sodium bicarbonate to determine available phosphorus (P) using the molybdenum antimony colorimetric method. Ammonium N contents were determined using the indophenol blue colorimetric method (Keeney and Nelson 1982). Nitrate contents were measured by dual-wavelength spectrometry (Norman et al. 1985). Total concentration of the metals was measured after digestion in a mixture of $H_2O_2$, $HNO_3$, and HCl (1:4:2, v/v) with a sealed digestion tank at 190 °C for 30 h. Metal concentrations were determined with an inductively coupled plasma–optical emission spectrometer (ICP–OES, Varian, 720-ES, USA). Potential ammonia oxidation (PAO) was measured according to the potassium chlorate inhibition nitrite oxidation method of Kurola et al. (2005). For the assay, 5 g (fresh weight) of soil was incubated in conical flask containing 50 mL of phosphate-buffered saline (g/l NaCl 8.0, KCl 0.2, $Na_2HPO_4$ 0.2, and $NaH_2PO_4$ 0.2 [pH 7.1]) and 50 mL of 5 mmol/L $(NH_4)_2SO_4$ in the dark

for 24 h on a shaker at 100 rpm at 25 °C. $KClO_3$ (final concentration 10 mg/L) was added to inhibit nitrite oxidation. Triplicate flasks for each treatment were incubated in the same condition. The potential ammonium oxidation activity was calculated as $NO_2^-$ production with per dry gram in per-hour mg ($NO_2^-$–N)/kg h.

### Real-Time PCR Assay

Genomic DNA was extracted from 0.5 g of soil using the Power Soil DNA kit (MoBio Laboratories, Solana Beach, California, USA) according to the manufacturer's protocol. The extracted DNA was then immediately stored at −20 °C. The archaeal and bacterial *amo*A genes were amplified with the primers as previously described (Francis et al. 2005; Rotthauwe et al. 1997), Arch-*amo*A-F (5′-CTAATGGTCTG GCTTAGACG-3′), Arch-*amo*A-R (5′-GCGGCCATCCAT CTGTATGT-3′), *amo*A-F (5′-GGGGTTTCTACTGGTG GT-3′), *amo*A-R (5′-CCCCTCTGGAAAGCCTTCTTC-3′) (Table S1). The q-PCR assays were performed in polypropylene 96-well plates on an ABI Prism 7500 sequence detection system (Applied Biosystems, USA). Each 20 μL of reaction contained the following: 10 μL of AB solute q-PCR Master Mix (AB Gene, USA), 1.0 μL of each primer (10 μM; Sangon Biotech, China), 1 μL of bovine serum albumin (10 mg/mL), 7 μL of $H_2O$, and 1 μL of template DNA (0.5 ng/μL). PCR conditions were as follows: 15 min at 95 °C, followed by 40 cycles of 95 °C for 15 s, 1 min at the annealing temperature, and 72 °C for 1 min. Each plate included triplicate reactions per DNA sample and the suitable standards set as follows.

Standard curves for real-time PCR assays were developed as previously described by He et al. (2007). Briefly, bacterial and archaeal *amo*A genes were PCR-amplified from the extracted DNA using the above-mentioned primer pairs Arch-*amo*A-F/Arch-*amo*A-R and *amo*A-F/*amo*A-R, and the PCR products were cloned into the ρMD l8-T Easy Vector. The resulting ligation products were used to transform *Escherichia coli* DH5α competent cells, and the positive clones were selected to extract the plasmid DNA with a plasmid purification kit (TaKaRa, China). The plasmid DNA concentration was determined on a NanoDrop spectrophotometer (NanoDrop Technologies, USA), and the copy numbers of the target genes were calculated from the concentration of the extracted plasmid DNA. Standard curves were generated from six tenfold dilutions of plasmid DNA, and the concentrations ranged from 100 to $10^{-4}$ ng. For all q-PCR assays, a linear relationship was noted between the log of the copy number and the calculated threshold cycle value ($R^2 > 0.99$ and amplification efficiency of 90–110 %). Melting-curve analysis of the PCR products was performed after each assay to confirm the specificity of the primers. The archaeal and bacterial *amo*A copy numbers per gram of dry soil represent the gene abundances of AOA and AOB.

### Amplified PCR and DGGE

The pairs of primers used for the DGGE analysis of the bacterial and archaeal *amo*A gene amplifications were Arch-*amo*A-F/Arch-*amo*A-R and *amo*A-F/*amo*A-R, and the processes are listed in Table S1. A GC clamp was attached to the forward primers to prevent the complete separation of the fragment during DGGE. DGGE were performed on 8 % (w/v) polyacrylamide gel containing different denaturant gradients (Table S1). Gel electrophoresis was performed at a constant voltage of 100 V at 60 °C for 12 h. The gels were stained with SYBR Green I, and the images were acquired by Red Personal Imaging System (ProteinSimple, USA). The DGGE profiles were normalized and analyzed using Quantity One software (version 4.6.7; Bio-Rad, California, USA).

### Cloning, Sequencing, Phylogenetic Analysis, and Sequence Accession Numbers

Numbered bands in the DGGE were cut and suspended in 20 μL of sterile water for 24 h and reamplified with the primers *amo*A-F/*amo*A-R and arch-*amo*AF/arch-*amo*AR. The purified reamplified PCR products were cloned into the ρMD l8-T Easy Vector, and the ligation products were then used to transform *E. coli* DH5α-competent cells. The positive clones were amplified using the above-mentioned primers using a GC clamp and checked by DGGE. The correct one was selected for sequencing. All sequences were aligned using ClustalX for *amo*A gene including the unknown gel band sequences and the most relevant sequences retrieved from GenBank, especially those from soil. Phylogenetic analyses were performed using MEGA version 5.1, and the neighbor-joining tree was constructed using Kimura two-parameter distance with 1000 replicates to produce bootstrap values. All *amo*A gene sequences were deposited in the GenBank nucleotide sequence database under accession nos. KF986280 to KF986302 for AOB and KF986272 to KF986279 for AOA.

### Multivariate Analysis

Band position and peak intensity data from the DGGE profiles for each sample were exported for further statistical analyses. The bands with relative contribution <1 % were discarded. To eliminate the disturbance of different units, the environmental factors were disposed by standardization and centralization processing, and community information were under centralization processing. Redundancy analyses (RDA) were performed according to the results of the detrended correspondence analyses to determine the multivariate relationship between the species–groups community compositions and environmental

factors. A Monte Carlo permutation reduced the model test based on 499 random permutations and was used to test the significance of the first canonical axis and all canonical axes together. Relationships between soil characteristics (i.e. WC, pH, available P, Corg, Nt, $NH_4^+$, and $NO_3^-$), potential ammonia oxidation, total metal content (i.e. Cu, Cd, Cr, and Zn), and *amo*A abundance were established as the Pearson correlation coefficients using a commercial software program SPSS (version 18.0; SPSS, Chicago, Illinois, USA).

## Results and Discussion

### Soil Basic Characteristics and Metal Analysis

The main soil characteristics (WC, pH, available P, Corg, Nt, $NH_4^+$, and $NO_3^-$) of the 14 sampling sites are listed in Table 1. The pH values changed slightly from 7.21 to 7.80, which was consistent with latest surveys in Beijing suburbs (pH 7.0–8.2). Soil WC ranged from 7.23 to 25.79 % reaching the lowest value in the desert zone. Moreover, Corg (1.26–5.81 g/kg), Nt (0.28–0.70 g/kg), and available P (0.23–1.56 mg/kg) reached the lowest value in this desert zone as well. The samples from the farmland had greater Corg and Nt values than those in the desert zone indicating the close correlation of the former with the long-term fertilization in farmland. Long-term application of chemical fertilizer can improve the contents of inactive organic matter and increase oxidative stability of soil organic carbon, thereby increasing the carbon (C) and N contents in the soil. The Corg and Nt values in planted forest soil are not much different from those in agricultural soil. This is because the planted forest was transformed from farmland and also had a long fertilization time previously. In addition, the various values of available P, $NH_4^+$, and $NO_3^-$ are likely due to the regional fertilizer habit.

The average contents of Cr and Cd were 4–5 times greater than the soil background values of Beijing (29.80 and 0.12 mg/kg, respectively; Table 1). The average Cu and Zn contents were twice as much as that of background (18.7 and 57.5 mg/kg, respectively; Table 1). The other metals (i.e. Pb, Ni, and Co) did not exceed the background value in the region (data not shown). According to the national background value in China (the primary standard of "Environmental Quality Standard for Soil GB15618-1995"), the average contents of Cr, Cu, and Cd exceeded the standard (90, 35, and 0.20 mg/kg, respectively), and Cd was twice to thrice beyond the standard. Zn concentration did not exceed the standard in all samples (100 mg/kg). The results indicated that the sampling sites were under varying degrees of pollution. Nemerow composite index, a widely used indicator of pollution and calculated as depicted by Wang (Wang et al. 2012), showed that the desert area was moderately polluted, whereas the others were in lightly polluted condition.

### Potential Ammonia Oxidation and Abundance of AOA and AOB Analysis

Potential ammonia oxidation rates varied greatly and ranged from 0.001 to 0.213 mg ($NO_2^-$–N)/kg h (Fig. 1). The lowest rates were found in desert samples. The SD and the highest rate came from the forest soil AP. The mean value of PAO in the desert zone were much lower (0.021 ($NO_2^-$–N)/kg h) than those in farmland and planted forest soil.

The abundance of AOA and AOB was determined as shown in Fig. 2. The log value of AOA *amoA* gene copy numbers per gram of dry soil ranged from 7.94 to 9.43, and the highest copy number was found in forest soil CP. The mean value of AOA in farmland is almost three times than in desert soil, and the mean value of AOA in planted forest soil is close to that of AOA in farmland. The log value of AOB *amo*A gene copy numbers per gram of dry soil ranged from 6.49 to 9.03, and the highest value appeared in forest soil AP. Both of the mean values of AOB in farmland and planted forest soil were >10 m times than in desert soil. The archaeal *amo*A gene copy numbers were greater than those of the bacterial *amo*A gene, and the ratios of AOA to AOB ranged from 1.21 to 12.98. This result gives evidence that AOA are present in high numbers in the heavy metal–contaminated soils of Miyun County. The desert area, which exhibited the lowest nutrient level and highest contamination, had the lowest bacterial and archaeal *amo*A copy numbers. Moreover, AOA in desert area had much greater numbers than AOB. The mean value of AOA/AOB (10.21) is much greater than in those in farmland and planted forest soil (3.39 and 3.44, respectively).

### Correlation Between PAO, AOA and AOB Abundance and Environmental Variables

The correlation between PAO and soil properties (Table 2) suggests that Corg, available P, and Nt have significant influence on AOA and AOB abundance and potential ammonia oxidation ($P < 0.05$). Soil characteristics (i.e. C, N, and P contents) are important factors that affect ammonia oxidation process at the regional level, and they have been verified in a considerable number of researches (Yao et al. 2013; He et al. 2007). The Pearson correlation also indicates that WC and $NH_4^+$ have a significant correlation with AOB ($P < 0.05$) and have no close relationship with AOA (Table 2), thus indicating that AOB is more susceptible to the effects of WC and $NH_4^+$ than AOA. Meanwhile, this result suggests that AOA is more adaptable to drought or a low-nitrogen environment than AOB.

**Table 1** Physicochemical characteristics and heavy-metal contents of soil samples[a]

| Sampling abbreviations | Land-use type | WC[1] (%) | PH | Available P (mg/kg) | Corg[1] (g/kg) | Nt[1] (g/kg) | $NH_4^+$ (mg/kg) | $NO_3^-$ (mg/kg) | Heavy-metal content (mg/kg) | | | |
|---|---|---|---|---|---|---|---|---|---|---|---|---|
| | | | | | | | | | Cr | Cu | Cd | Zn |
| FD | Desert | 13.03 (±0.51) | 7.75 (±0.21) | 1.35 (±0.02) | 1.26 (±0.03) | 0.28 (±0.01) | 0.61 (±0.02) | 0.09 (±0.003) | 74.27 (±1.36) | 46.21 (±1.20) | 0.65 (±0.12) | 76.64 (±2.12) |
| SD | Desert | 7.23 (±0.22) | 7.21 (±0.14) | 0.23 (±0.01) | 1.83 (±0.04) | 0.29 (±0.01) | 2.83 (±0.09) | 0.05 (±0.001) | 98.30 (±2.43) | 59.91 (±4.66) | 0.61 (±0.09) | 96.16 (±3.87) |
| XD | Desert | 8.67 (±0.21) | 7.24 (±0.22) | 1.01 (±0.02) | 3.39 (±0.10) | 0.55 (±0.01) | 6.03 (±0.21) | 0.89 (±0.02) | 117.09 (±4.61) | 41.27 (±2.35) | 0.68 (±0.10) | 85.78 (±4.73) |
| HD | Desert | 9.51 (±0.25) | 7.67 (±0.31) | 1.56 (±0.03) | 5.81 (±0.12) | 0.70 (±0.02) | 0.01 (±0.001) | 8.39 (±0.31) | 118.22 (±4.01) | 42.60 (±2.90) | 0.78 (±0.21) | 101.94 (±6.19) |
| AF | Farmland | 12.14 (±0.34) | 7.80 (±0.12) | 8.23 (±0.31) | 6.99 (±0.12) | 1.19 (±0.03) | 0.02 (±0.001) | 23.85 (±0.88) | 120.15 (±5.09) | 35.76 (±1.36) | 0.48 (±0.11) | 85.47 (±3.25) |
| AP | Planted forest | 17.94 (±0.53) | 7.26 (±0.30) | 38.67 (±1.67) | 10.11 (±0.18) | 1.37 (±0.03) | 0.95 (±0.02) | 43.82 (±1.45) | 106.33 (±4.55) | 26.84 (±1.07) | 0.39 (±0.13) | 90.70 (±3.29) |
| BF | Farmland | 19.34 (±0.71) | 7.45 (±0.20) | 21.55 (±0.92) | 13.82 (±0.20) | 1.40 (±0.04) | 0.01 (±0.001) | 13.80 (±0.47) | 221.64 (±7.03) | 40.29 (±2.31) | 0.46 (±0.08) | 116.94 (±5.40) |
| BP | Planted forest | 11.20 (±0.31) | 7.32 (±0.42) | 0.67 (±0.02) | 7.54 (±0.12) | 0.75 (±0.01) | 5.48 (±0.20) | 0.10 (±0.006) | 174.46 (±6.50) | 52.27 (±1.92) | 0.48 (±0.11) | 124.16 (±5.89) |
| CF | Farmland | 14.71 (±0.42) | 7.47 (±0.26) | 65.93 (±2.35) | 11.78 (±0.16) | 1.54 (±0.02) | 1.17 (±0.04) | 3.25 (±0.14) | 302.96 (±10.22) | 36.72 (±1.32) | 0.39 (±0.07) | 112.49 (±3.70) |
| CP | Planted forest | 14.76 (±0.40) | 7.73 (±0.24) | 23.18 (±1.09) | 11.19 (±0.15) | 1.24 (±0.02) | 0.95 (±0.04) | 17.95 (±0.72) | 187.58 (±7.24) | 26.68 (±1.04) | 0.48 (±0.13) | 83.89 (±4.52) |
| DF | Farmland | 25.79 (±0.81) | 7.65 (±0.12) | 21.77 (±0.98) | 7.50 (±0.05) | 0.94 (±0.02) | 7.41 (±0.23) | 4.99 (±0.20) | 90.19 (±4.25) | 28.90 (±1.09) | 0.43 (±0.20) | 96.10 (±4.39) |
| DP | Planted Forest | 21.76 (±0.80) | 7.70 (±0.32) | 6.10 (±0.26) | 9.42 (±0.06) | 1.54 (±0.03) | 1.22 (±0.03) | 5.54 (±0.31) | 80.22 (±2.44) | 20.86 (±0.98) | 0.45 (±0.21) | 73.29 (±3.79) |
| EF | Farmland | 22.45 (±0.89) | 7.60 (±0.14) | 25.50 (±1.21) | 7.80 (±0.05) | 1.15 (±0.02) | 15.27 (±0.45) | 9.13 (±0.54) | 186.16 (±6.90) | 24.73 (±1.24) | 0.50 (±0.17) | 77.43 (±4.02) |
| EP | Planted forest | 22.18 (±0.86) | 7.57 (±0.36) | 11.77 (±0.43) | 13.12 (±0.19) | 1.49 (±0.03) | 1.33 (±0.01) | 20.73 (±0.89) | 97.67 (±4.29) | 25.72 (±1.33) | 0.50 (±0.19) | 89.11 (±4.29) |
| The average in iron area | | | | | | | | | 141.09 | 36.34 | 0.52 | 93.58 |
| Soil background in Beijing | | | | | | | | | 29.80 | 18.7 | 0.12 | 57.5 |
| National soil background | | | | | | | | | 90 | 35 | 0.20 | 100 |

*WC* Water content, *Corg* organic C, *Nt* total nitrogen

[a] Values represent average ± SD

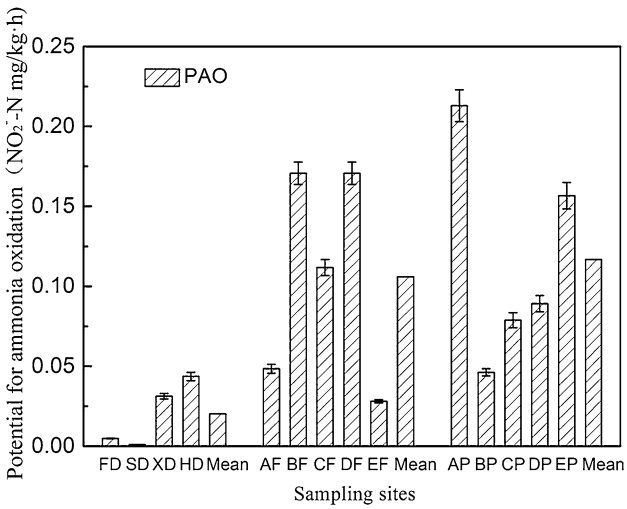


**Fig. 1** Changes in potential for ammonia oxidation rates of the different sampling sites. Samples FD, SD, XD, HD came from desert area, samples AF, BF, CF, DF, EF came from farmland soil whereas AP, BP, CP, DP, EP came from planted forest soil. *Bars* represent the standard errors of three independent measurements

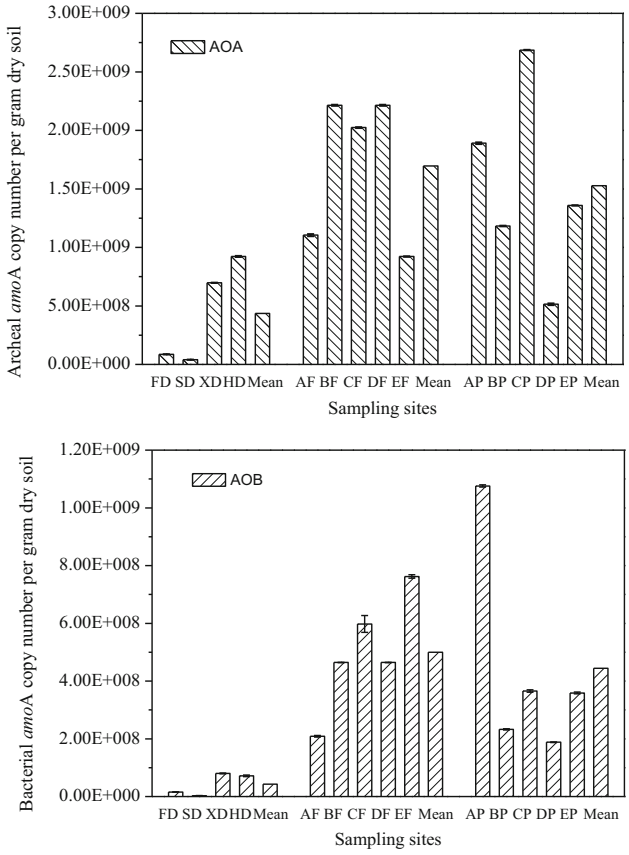


**Fig. 2** Changes in *amo*A gene copies of the different sampling sites. *Bars* represent the standard errors of triplicate reactions of the same sample

Some studies have confirmed this conclusion (Placella and Firestone 2013; Verhamme et al. 2011), and the extensive adaptability of AOA may explain why AOA had much greater numbers than AOB and occupied the main ecological niche of ammonia oxidizing process in the desert area. AOA and AOB abundance had a close relationship with PAO ($r = 0.642$, $P < 0.01$ and $r = 0.551$ $P < 0.05$ [Table 2]) indicating that both AOA and AOB play dominant roles in ammoxidation in the whole region.

To determine the independent effects of heavy-metal pollution on ammonia oxidizer, partial correlation between metal, PAO, and ammonia oxidizer abundance was performed (Table 3). Cu and Cd concentrations had effects on the abundance of AOA ($r = -0.653$, $P < 0.05$; $r = -0.664$, $P < 0.05$) but had no direct relationship with AOB. Although Cu and Cd have a certain inhibitory effect on AOA abundance, AOA copy number were much greater than AOB indicating that slight heavy-metal pollution in study area is not enough to change the niches occupied by AOA and AOB in the ammonia-oxidation process. In addition, long-term interference of Cr did not change the abundance of soil ammonia oxidizer, but it inhibited the ammonia-oxidation rate.

## Genetic Profiling of Bacterial and Archaeal *amo*A Genes

The community structure of AOB and AOA were analyzed by DGGE (Figs. S1a, b). DGGE analysis could show the dominant species that can be amplified by the selected primers, but by no means does it represents the entire community. Repeated DGGE analyses resulted in highly reproducible patterns (data not shown). DGGE profile of AOB showed a marked difference between different samples: A total of 23 bands were observed (Fig. S1a). Bands C9 and C12–C15 appeared in the profiles of most samples, and bands C12 and C13 showed high intensity in most samples. The samples from the tailing area had lower Shannon–Wiener indices and richness values of AOB (Table S2). The DGGE patterns of AOA showed remarkable difference with the AOB profile, and only eight bands were detected (Fig. S1b). Bands C1–C3 were detected in most samples with greater intensity than the other bands. The richness of AOA showed significantly lower values than those of AOB (Table S2).

The sequences at 5 % nucleotide cut-offs were used to construct the phylogenetic trees (Mosier and Francis 2008). The bacterial *amo*A gene sequences can be grouped into three clusters (Fig. 3). Most bands located in the lower part of the gel were grouped with *Nitrosospira briensis* (Purkhold et al. 2003), *Nitrosospira* sp. LT2FB (Mintie et al. 2003), and *N. multiformis* (Norton et al. 2002) and

**Table 2** Correlation between soil physicochemical characteristics and *amo*A abundance and potential ammonia-oxidation rate

| | WC | PH | AP | Corg | Nt | $NH_4^+$ | $NO_3^-$ | PAO | AOB | AOA | AOA/AOB |
|---|---|---|---|---|---|---|---|---|---|---|---|
| PAO | 0.357 | −0.147 | 0.685** | 0.774** | 0.779** | −0.375 | 0.636* | 1 | | | |
| AOB | 0.662** | −0.439 | 0.656* | 0.532* | 0.534* | 0.607* | 0.580* | 0.551* | 1 | | |
| AOA | 0.248 | −0.194 | 0.698** | 0.810** | 0.675** | −0.212 | 0.472 | 0.672** | 0.528 | 1 | |
| AOA/AOB | −0.565* | 0.022 | −0.160 | −0.014 | −0.086 | −0.224 | −0.134 | −0.065 | −0.499 | 0.268 | 1 |

* $P < 0.05$ (two-tailed); ** $P < 0.01$ (two-tailed)

**Table 3** Partial correlation between metal contents and *amo*A abundance and potential ammonia-oxidation rate

| | Cr | Cu | Cd | Zn |
|---|---|---|---|---|
| AO | −0.607* | −0.047 | 0.125 | −0.078 |
| AOB | 0.078 | −0.195 | 0.277 | 0.353 |
| AOA | 0.111 | −0.653* | −0.664* | −0.368 |
| AOA/AOB | −0.216 | −0.669** | 0.034 | −0.606* |

* $P < 0.05$ (two-tailed); ** $P < 0.01$ (two-tailed)

thus belonged to *Nitrosospira* cluster three. Several bands (1 through 6, 8 11, C9, and C12) were related with two *Nitrosomonadales* species from paddy soil and Yangtze Estuary sediments (Wu et al. 2011; Zheng et al. 2014) and were recognized as *Nitrosomonadales*-like sequences. Most of the AOB *amoA* OTUs belongs to cluster three (63 OTUs, 61 %), which the most dominant cluster. The dominance of *Nitrosospira* was already reported in earlier studies showing that *Nitrosospira* was the majority species in soil ecosystems (Chen et al. 2011; Xu et al. 2012; Wang et al. 2013) including riparian or agricultural soil sampled from the watershed of the Miyun reservoir. Furthermore, the dominance of *Nitrosospira* were also verified in Cu- or Zn-contaminated soil by Mertens et al. (2009) and Liu et al. (2014).

The phylogenetic analysis of the archaeal *amo*A gene shown that all selected clones can be divided into two clusters, i.e. group 1.1a-associated and 1.1b-associated (Fig. 4). Only three rare DGGE bands (four through six) were placed in group 1.1a-associated because they had high similarity with the sequences in group 1.1a, which came from the marine environment (Hallam et al. 2006; Jung et al. 2011; Könneke et al. 2005; Lehtovirta-Morley et al. 2011; Matsutani et al. 2011). The majority of AOA sequences were grouped with *Candidatus Nitrososphaera gargensis* (Hatzenpichler et al. 2008) and *C. Nitrososphaera* sp. EN76 (Tourna et al. 2011) and thus belonged to group 1.1b indicating that group1.1b dominated the AOA community. This result was consistent with some surveys showing that the AOA community was mainly dominated by group 1.1b in neutral and alkaline soil, whereas group 1.1a-associated was mainly distributed in acidic soil (He et al. 2007; Shen et al. 2008, 2012).

## Relationships Between Environmental Variables and Ammonia-Oxidizer Community Structure

RDA was performed to identify the parameters that induce changes in the ammonia-oxidizer community structure. The Monte Carlo tests for the first and all canonical axes were highly significant ($P < 0.01$) indicating that these soil parameters are important in explaining the microbial community compositions. The first two canonical axes from the RDA of bacterial *amo*A DGGE fingerprints explained 31.7 and 16.0 % of the variation in the species data and accounted for 34.3 and 17.3 % of the cumulative variance of the species-environmental relation (Fig. 5). The variable that correlated most strongly with RDA 1 was $NH_4^+$ contents ($P < 0.01$), whereas Corg, Nt, available P, WC, and Cd contents ($P < 0.05$) correlated best with RDA 2. Those factors were proposed to contribute the most to AOB community composition. Moreover, except for EF, samples from the farmland soil were grouped together (Fig. 5a), and the samples from deserts and planted forest soil presented similar phenomenon indicating that soil type had significant influence on the AOB community structure.

The first two axes from the RDA of the AOA DGGE fingerprints explained 70.2 % of the total cumulative species data variance and accounted for 74.6 % of the cumulative variance of the species-environmental relationship (Fig. 6). $NH_4^+$ contents was the only variable that correlated strongly with RDA 1 ($P < 0.01$), whereas the variable correlated best with RDA 2 ($P < 0.05$) was water contents. These results indicated that AOA community structure may be significantly affected by soil characteristics and that heavy-metal interference did not have an obvious inhibitory effect on the AOA community.

## Local Factors Affecting AOA and AOB

Mantel test was performed to analyze the local environmental factors controlling the abundance and community structure of AOA and AOB (Table 4). Results show that

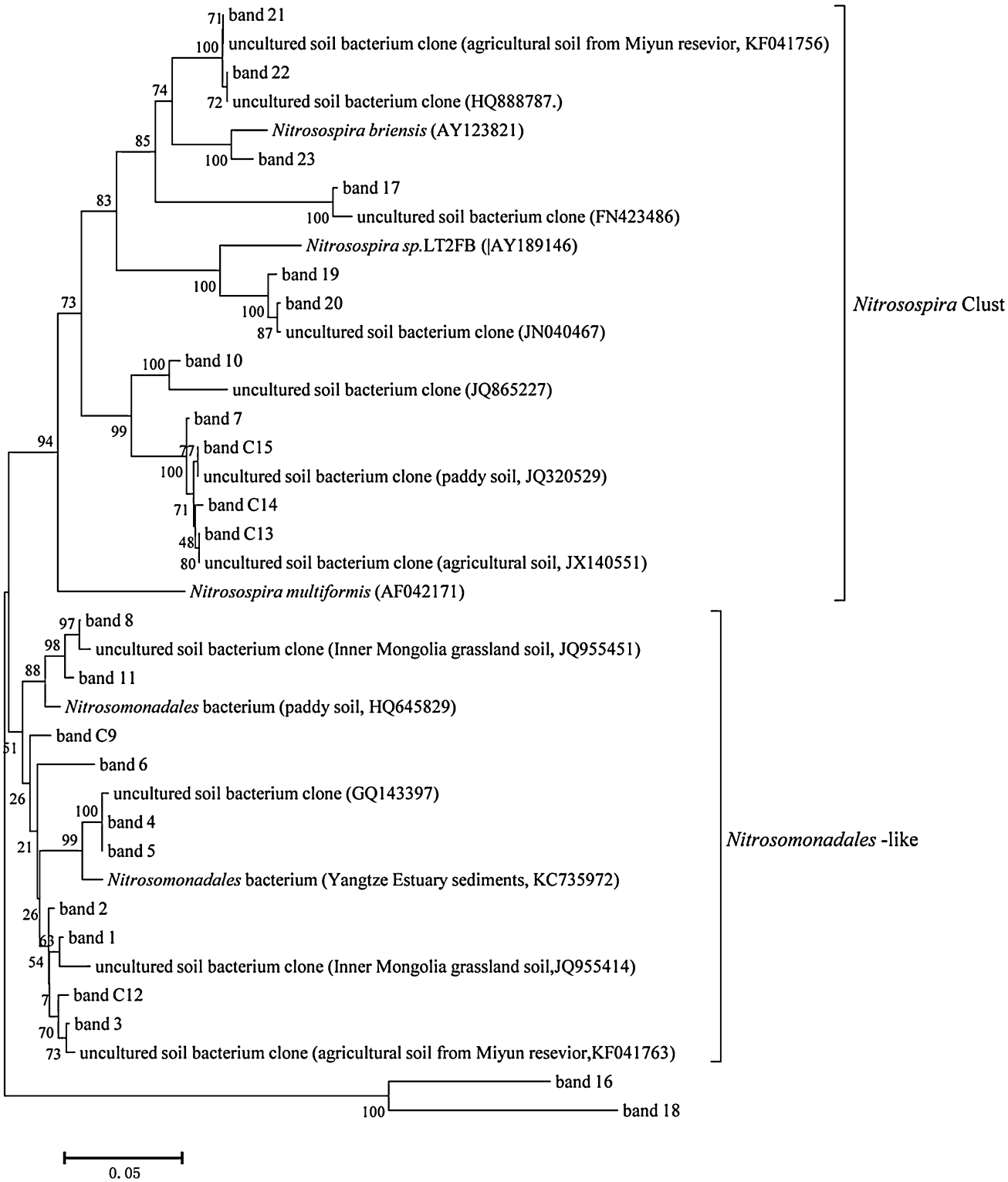


**Fig. 3** Phylogenetic tree of the bacterial *amo*A gene sequences in this study and some relevant sequences retrieved from GenBank that were reconstructed using neighbor-joining method in MEGA 5.1. The significant bootstrap values (>50) at the nodes represent the reliable support for the clusters. *Scale bar* represents 5 % nucleotide substitution

soil properties have a significant correlation with AOA and AOB (Mantel $r = 0.3183$, $P < 0.05$; Mantel $r = 0.4659$, $P < 0.05$), whereas only AOA has close relation with heavy metal (Mental $r = 0.3568$, $P < 0.05$) indicating that soil properties play more important roles in shaping the local ammonia-oxidizer community. Both RDA and

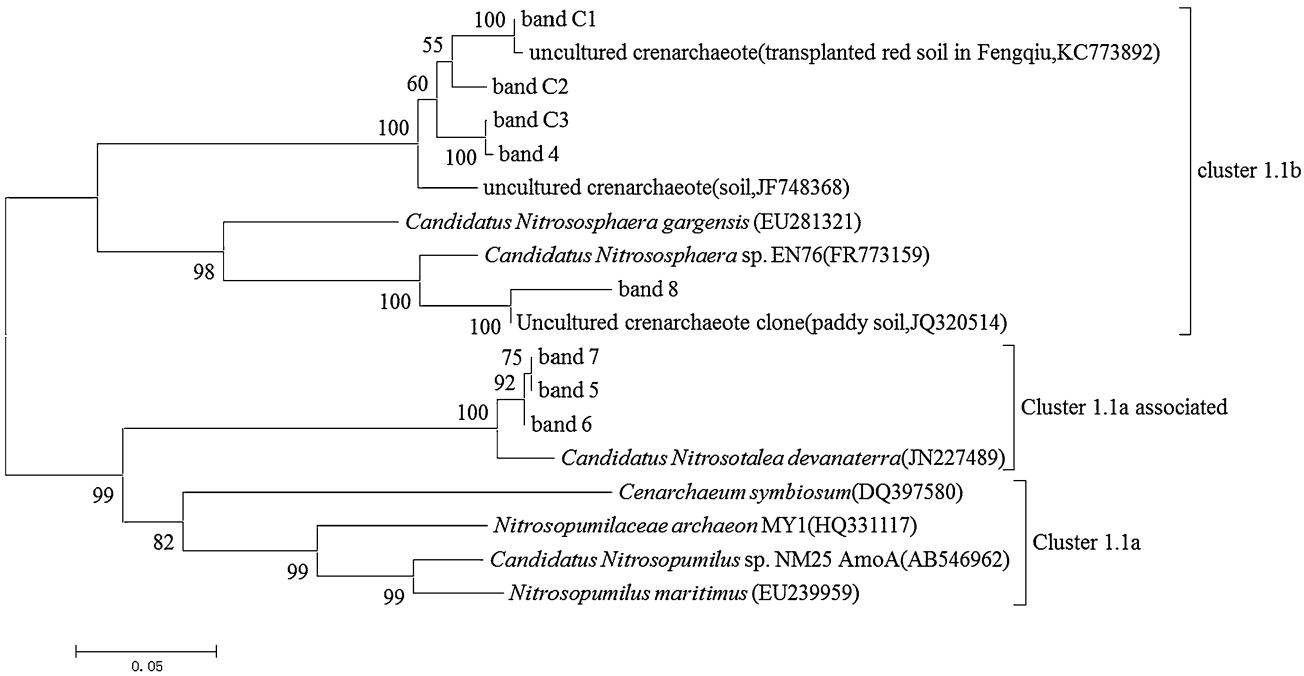


**Fig. 4** Phylogenetic tree of the archaeal *amo*A gene sequences in this study and some relevant sequences retrieved from GenBank which were reconstructed using neighbor-joining method in MEGA 5.1. The significant bootstrap values (>50) at the nodes represent the reliable support for clusters. *Scale bar* represents 5 % nucleotide substitution

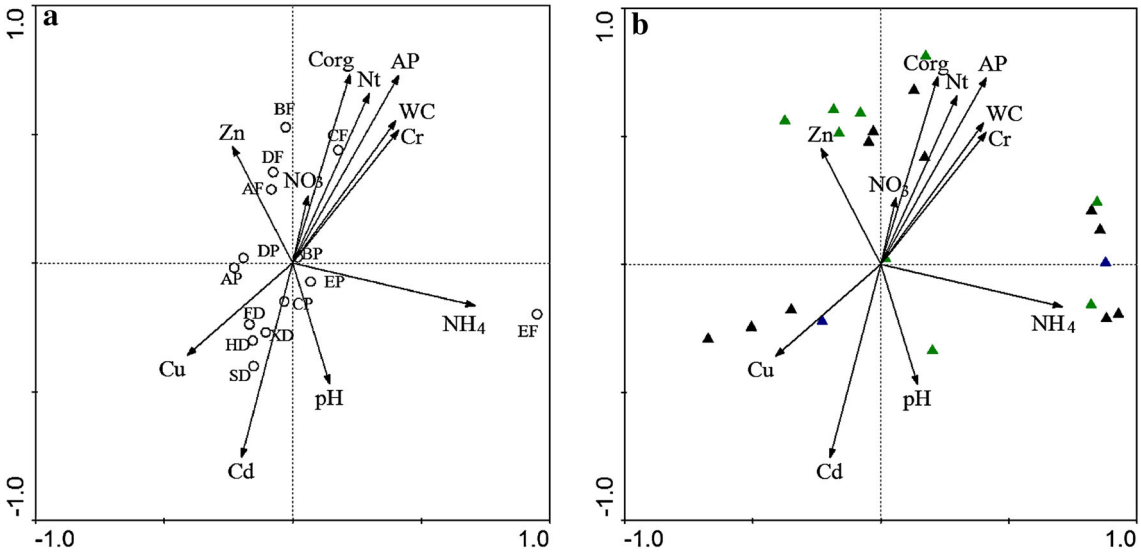


**Fig. 5** RDA ordination plot showing the relationship between the distribution of AOB composition and soil characteristics and heavy metal. **a** correlation between environmental variables and samples; **b** correlation between environmental variables and species. The variables were denoted by *solid lines with filled arrows*. The *triangles* indicate the ammonia oxidizing bacteria species, and the *black triangle* for *Nitrosospira* cluster three, *green triangle* for cluster *Nitrosomonadales*-like, and *blue triangle* for band 16 and 18. *Open circles* represent the sampling sites (Color figure online)

Pearson correlation showed that $NH_4^+$ as a substrate contributes the most to the abundance and community structure of AOA and AOB. Meanwhile, organic matter, N, and available P could provide essential elements for ammonia-oxidizing microorganism growth. In addition, soil water contents, as an important factor that has a close relation with soil substrate or oxygen concentration, could significantly affect ammonia oxidizers.

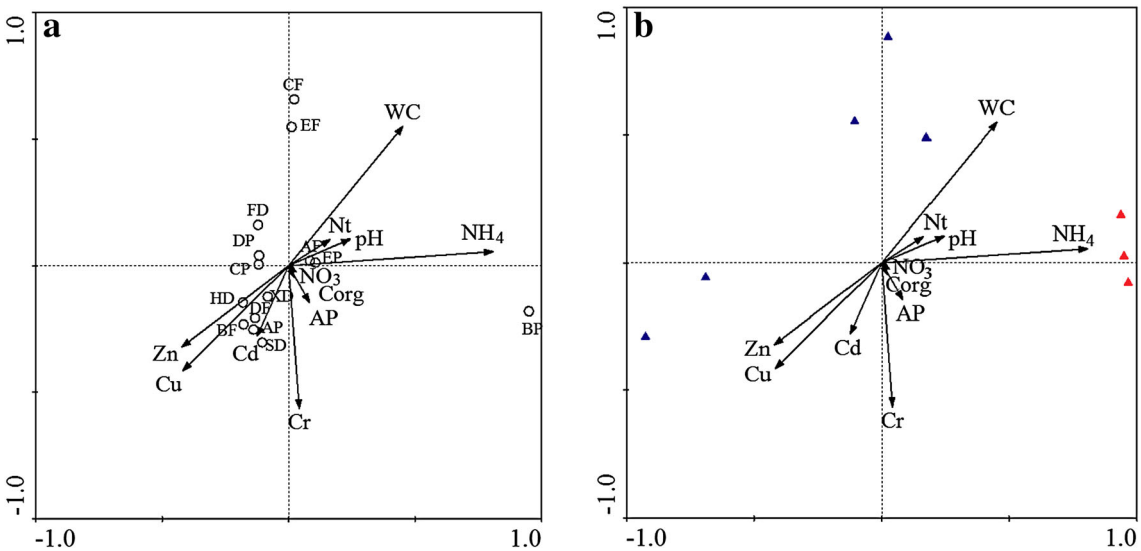


**Fig. 6** RDA ordination plot showing the relationship between the distribution of AOA composition and soil characteristics and heavy metal. **a** correlation between environmental variables and samples; **b** correlation between environmental variables and species. The variables were denoted by *solid lines with filled arrows*. *Triangles* indicate the AOB species and the *red triangle* for the species in group 1.1a, whereas the *black triangle* is for group 1.1b. *Open circles* represent the sampling sites (Color figure online)

**Table 4** Mantel statistic based on Pearson's product-moment correlation indicating the relationship between the AOA or AOB and soil properties or heavy metals[a]

| | AOA | | AOB | |
|---|---|---|---|---|
| | Mentel *r* | *P* | Mentel *r* | *P* |
| Soil | 0.3183 | 0.0451* | 0.4659 | 0.0168* |
| Heavy metal | 0.3568 | 0.0284* | −0.06582 | 0.5794 |

[a] Analysis was based on 9999 random permutations

* $P < 0.05$; ** $P < 0.01$

Although multiple soil characteristics play important roles in the abundance and community composition of AOA and AOB, the effect of heavy metals should not be ignored (Table 3; Fig. 5). For example, Cu significantly inhibited the abundance of AOA ($r = -0.653$*, $P < 0.05$) and had no obvious effect on AOB abundance. The energy metabolism of AOA is dependent on the electronic transport system containing Cu instead of Fe, which may affect the sensitivity of the AOA to Cu (Walker et al. 2010). Cd significantly affected the AOB community structure, but it did not change the AOB abundance. This is probably because some AOB species generated tolerance mechanisms to Cd increased, whereas susceptible ones reduced or disappeared. Cd pollution changed the diversity of AOB and significantly decreased AOA abundance, thus indicating that Cd pollution has a certain effect on ammonia oxidizer. The long-term Cr interference did not change the abundance and community structure of ammonia oxidizers, whereas it obviously inhibited the potential ammonia-oxidation rates (Table 3; $r = -0.607$*, $P < 0.05$). We hypothesize that the possible ways by which Cr affects PAO are to inhibit the transcription and synthesis of *amo*A mRNA after breaking into the microbial cell, thereby cause gradual decrease in the functional enzyme concentration and ultimately affect the ammonia-oxidation process.

## Conclusions

The diversity and abundance of AOA and AOB in an iron-mining area were analyzed by employing a functional genetic marker *amo*A gene. AOA are more abundant than AOB, and AOA may have a dominant role in ammonia-oxidizing progress in the whole region. Multiple soil characteristics play important roles in the abundance and community composition of AOA and AOB. The inhibition of heavy metals did not change the niches of AOA and AOB. But heavy metals (i.e. Cd, Cu, and Zn) had a certain influence on the community structure of AOB. Interestingly, Cr did not affect the ammonia oxidizer, but it inhibited the potential ammonia-oxidation rate. Therefore, heavy-metal pollution in this iron-mining area hindered the soil nitrogen cycle to some extent and may affect local soil fertility.

**Acknowledgments** This work was supported by the National Natural Science Foundation of China (Grant No. 41273091), Beijing Nova Program (Grant No. Z111106054511043), International Joint Key Project from Chinese Ministry of Science and Technology (Grant No. 2010DFA12780), National Outstanding Youth Research Foundation of China (Grant No. 40925010), International Joint Key Project

from National Natural Science Foundation of China (Grant No. 40920134003), and National Natural Science Foundation of China (Grant No. 41273092).

## References

Broos K, Mertens J, Smolders E (2005) Toxicity of heavy metals in soil assessed with various soil microbial and plant growth assays: a comparative study. Environ Toxicol Chem 24:634–640

Chen X, Zhang LM, Shen JP, Wei WX, He JZ (2011) Abundance and community structure of ammonia-oxidizing archaea and bacteria in an acid paddy soil. Biol Fertil Soils 47:323–331

Di H, Cameron K, Shen JP, Winefield C, O'Callaghan M, Bowatte S et al (2009) Nitrification driven by bacteria and not archaea in nitrogen-rich grassland soils. Nat Geosci 2:621–624

Erguder TH, Boon N, Wittebolle L, Marzorati M, Verstraete W (2009) Environmental factors shaping the ecological niches of ammonia-oxidizing archaea. FEMS Microbiol Rev 33:855–869

Francis CA, Roberts KJ, Beman JM, Santoro AE, Oakley BB (2005) Ubiquity and diversity of ammonia-oxidizing archaea in water columns and sediments of the ocean. Proc Natl Acad Sci USA 102:14683–14688

Gubry-Rangin C, Hai B, Quince C, Engel M, Thomson BC, James P et al (2011) Niche specialization of terrestrial archaeal ammonia oxidizers. Proc Natl Acad Sci USA 108:21206–21211

Hallam SJ, Mincer TJ, Schleper C, Preston CM, Roberts K et al (2006) Pathways of carbon assimilation and ammonia oxidation suggested by environmental genomic analyses of marine *Crenarchaeota*. PLoS Biol 4:e95

Hatzenpichler R, Lebedeva EV, Spieck E, Stoecker K, Richter A et al (2008) A moderately thermophilic ammonia-oxidizing crenarchaeote from a hot spring. Proc Natl Acad Sci USA 105:2134–2139

He JZ, Shen JP, Zhang LM, Zhu YG, Zheng YM et al (2007) Quantitative analyses of the abundance and composition of ammonia-oxidizing bacteria and ammonia-oxidizing archaea of a Chinese upland red soil under long-term fertilization practices. Environ Microbiol 9:2364–2374

Jia Z, Conrad R (2009) Bacteria rather than Archaea dominate microbial ammonia oxidation in an agricultural soil. Environ Microbiol 11:1658–1671

Jung MY, Park SJ, Min D, Kim JS, Rijpstra WIC et al (2011) Enrichment and characterization of an autotrophic ammonia-oxidizing archaeon of mesophilic crenarchaeal group 1.1a from an agricultural soil. Appl Environ Microbiol 77(24):8635–8647

Keeney D, Nelson D (1982) Nitrogen—inorganic forms. In: Page AL (ed) Methods of soil analysis: part 2—chemical and microbiological properties. Soil Sci Soc Am, Madison, pp 643–698

Kelly JJ, Policht K, Grancharova T, Hundal LS (2011) Distinct responses in ammonia-oxidizing archaea and bacteria after addition of biosolids to an agricultural soil. Appl Environ Microbiol 77:6551–6558

Kurola J, SalkinojaSlonen M, Aarnio T, Hultman J, Romantschuk M (2005) Activity, diversity and population size of ammonia-oxidising bacteria in oil-contaminated landfarming soil. FEMS Microbiol Lett 250:33–38

Lehtovirta-Morley LE, Stoecker K, Vilcinskas A, Prosser JI, Nicol GW (2011) Cultivation of an obligate acidophilic ammonia oxidizer from a nitrifying acid soil. Proc Natl Acad Sci USA 108:15892–15897

Liu Y, Liu YZ, Ding Y, Zheng J, Zhou T et al (2014) Abundance, composition and activity of ammonia oxidizer and denitrifier communities in metal polluted rice paddies from South China. PLoS One 7:e102000

Matsutani N, Nakagawa T, Nakamura K, Takahashi R, Yoshihara K, Tokuyama T (2011) Enrichment of a novel marine ammonia-oxidizing archaeon obtained from sand of an eelgrass zone. Microbes Environ 26:23–29

Mertens J, Broos K, Wakelin SA, Kowalchuk GA, Springael D, Smolders E (2009) Bacteria, not archaea, restore nitrification in a zinc-contaminated soil. ISME J 3:916–923

Mintie A, Heichen R, Cromack K Jr, Myrold D, Bottomley P (2003) Ammonia-oxidizing bacteria along meadow-to-forest transects in the Oregon Cascade Mountains. Appl Environ Microbiol 69:3129–3136

Morel F, Price N (2003) The biogeochemical cycles of trace metals in the oceans. Science 300:944–947

Mosier AC, Francis CA (2008) Relative abundance and diversity of ammonia-oxidizing archaea and bacteria in the San Francisco Bay estuary. Environ Microbiol 11:3002–3016

Norman RJ, Edberg JC, Stucki JW (1985) Determination of nitrate in soil extracts by dual-wavelength ultraviolet spectrophotometry. Soil Sci Soc Am J 49:1182–1185

Norton JM, Alzerreca JJ, Suwa Y, Klotz MG (2002) Diversity of ammonia monooxygenase operon in autotrophic ammonia-oxidizing bacteria. Arch Microbiol 177:139–149

O'Sullivan C, Wakelin S, Fillery I, Roper M (2013) Factors affecting ammonia oxidizing micro-organisms and potential nitrification rates in southern Australian agricultural soils. Soil Res 51:240–252

Placella SA, Firestone MK (2013) Transcriptional response of nitrifying communities to wetting of dry soil. Appl Environ Microbiol 79:3294–3302

Purkhold U, Wagner M, Timmermann G, Pommerening-Röser A, Koops HP (2003) 16S rRNA and *amo*A-based phylogeny of 12 novel betaproteobacterial ammonia-oxidizing isolates: extension of the dataset and proposal of a new lineage within the nitrosomonads. Int J Syst Evol Microbiol 53:1485–1494

Qin H, Yuan H, Zhang H, Zhu Y, Yin C et al (2013) Ammonia-oxidizing archaea are more important than ammonia-oxidizing bacteria in nitrification and $NO_3^-$–N loss in acidic soil of sloped land. Biol Fertil Soils 49:767–776

Rotthauwe JH, Witzel K-P, Liesack W (1997) The ammonia monooxygenase structural gene *amo*A as a functional marker: molecular fine-scale analysis of natural ammonia-oxidizing populations. Appl Environ Microbiol 63:4704–4712

Ruyters S, Nicol GW, Prosser JI, Lievens B, Smolders E (2013) Activity of the ammonia oxidising bacteria is responsible for zinc tolerance development of the ammonia oxidising community in soil: a stable isotope probing study. Soil Biol Biochem 58:244–247

Shen JP, Zhang LM, Zhu YG, Zhang JB, He JZ (2008) Abundance and composition of ammonia-oxidizing bacteria and ammonia-oxidizing archaea communities of an alkaline sandy loam. Environ Microbiol 10:1601–1611

Shen JP, Zhang LM, Di HJ, He JZ (2012) A review of ammonia-oxidizing bacteria and archaea in Chinese soils. Front Microbiol 3:296–331

Sher Y, Zaady E, Nejidat A (2013) Spatial and temporal diversity and abundance of ammonia oxidizers in semi-arid and arid soils: indications for a differential seasonal effect on archaeal and bacterial ammonia oxidizers. FEMS Microbiol Ecol 86:544–556

Tourna M, Stieglmeier M, Spang A, Könneke M, Schintlmeister A et al (2011) *Nitrososphaera viennensis*, an ammonia oxidizing archaeon from soil. Proc Natl Acad Sci USA 108:8420–8425

Verhamme DT, Prosser JI, Nicol GW (2011) Ammonia concentration determines differential growth of ammonia-oxidising archaea and bacteria in soil microcosms. ISME J 5:1067–1071

Walker C, De La Torre J, Klotz M, Urakawa H et al (2010) *Nitrosopumilus maritimus* genome reveals unique mechanisms

for nitrification and autotrophy in globally distributed marine crenarchaea. Proc Natl Acad Sci USA 107:8818–8823

Wang Q, Wang R, Tian C, Yu Y, Zhang Y, Dai J (2012) Using microbial community functioning as the complementary environmental condition indicator: a case study of an iron deposit tailing area. Eur J Soil Biol 51:22–29

Wang X, Wang C, Bao L, Xie S (2013) Abundance and community structure of ammonia-oxidizing microorganisms in reservoir sediment and adjacent soils. Appl Microbiol Biotechnol 98:1883–1992

Wu Y, Lu L, Wang B, Lin X, Zhu J et al (2011) Long-term field fertilization significantly alters community structure of ammonia-oxidizing bacteria rather than archaea in a paddy soil. Soil Sci Soc Am J 75:1431–1439

Xu YG, Yu WT, Ma Q, Zhou H (2012) Responses of bacterial and archaeal ammonia oxidisers of an acidic luvisols soil to different nitrogen fertilization rates after 9 years. Biol Fertil Soils 48: 827–837

Yao H, Campbell CD, Chapman SJ, Freitag TE, Nicol GW, Singh BK (2013) Multi-factorial drivers of ammonia oxidizer communities: evidence from a national soil survey. Environ Microbiol 15:2545–2556

Zheng Y, Hou L, Newell S, Liu M, Zhou J et al (2014) Community dynamics and activity of ammonia-oxidizing prokaryotes in intertidal sediments of the Yangtze estuary. Appl Environ Microbiol 80:408–419

Zhou M, Liao B, Shu W, Yang B, Lan C (2015) Pollution assessment and potential sources of heavy metals in agricultural soils around four Pb/Zn mines of Shaoguan City, China. Soil Sed Contam 24:76–89